International Journal of Mechanical Sciences 55 (2012) 22–29

Contents lists available at SciVerse ScienceDirect

International Journal of Mechanical Sciences

journal homepage: www.elsevier.com/locate/ijmecsci

Force and displacement transmissibility of a nonlinear isolator with high-static-low-dynamic-stiffness

A. Carrella [a,*], M.J. Brennan [b], T.P. Waters [c], V. Lopes Jr. [b]

[a] Queen's School of Engineering, BLADE, University of Bristol, Bristol BS8 1TR, UK
[b] Department of Mechanical Engineering, Universidade Estadual Paulista—UNESP/Ilha Solteira, Av. Brasil 5385-000, Ilha Solteira, Brazil
[c] Institute of Sound and Vibration Research, University of Southampton, Southampton SO17 1BJ, UK

ARTICLE INFO

Article history:
Received 28 June 2010
Received in revised form
26 October 2011
Accepted 24 November 2011
Available online 3 December 2011

Keywords:
Vibration isolation
Nonlinear stiffness
Duffing equation
Nonlinear transmissibility
HSDLS

ABSTRACT

Engineers often face the challenge of reducing the level of vibrations experienced by a given payload or those transmitted to the support structure to which a vibrating source is attached. In order to increase the range over which vibrations are isolated, soft mounts are often used in practice. The drawback of this approach is the static displacement may be too large for reasons of available space for example. Ideally, a vibration isolator should have a high-static stiffness, to withstand static loads without too large a displacement, and at the same time, a low dynamic stiffness so that the natural frequency of the system is as low as possible which will result in an increased isolation region. These two effects are mutually exclusive in linear isolators but can be overcome if properly configured nonlinear isolators are used. This paper is concerned with the characterisation of such a nonlinear isolator comprising three springs, two of which are configured to reduce the dynamic stiffness of the isolator. The dynamic behaviour of the isolator supporting a lumped mass is investigated using force and displacement transmissibility, which are derived by modelling the dynamic system as a single-degree-of-freedom system. This results in the system dynamics being approximately described by the Duffing equation. For a linear isolator, the dynamics of the system are the same regardless if the source of the excitation is a harmonic force acting on the payload (force transmissibility) or a harmonic motion of the base (displacement transmissibility) on which the payload is mounted. In this paper these two expressions are compared for the nonlinear isolator and it is shown that they differ. A particular feature of the displacement transmissibility is that the response is unbounded at the nonlinear resonance frequency unless the damping in the isolator is greater than some threshold value, which is not the case for force transmissibility. An explanation for this is offered in the paper.

1. Introduction

A recurrent problem in many engineering applications is that of preventing vibrations to be transmitted: most generally, there are two categories of problems: (i) the source of vibration is the payload itself, in which case the intention is to prevent the vibrations to be transmitted to its host structure, or (ii) the disturbance to the payload is caused by vibration of the host structure and the goal is to minimise the transmitted vibration. The former case is referred to in the literature as the force transmissibility problem, whilst the second as the displacement transmissibility problem. The non-dimensional parameter which is used to quantify the effectiveness of the isolation system is the transmissibility. For the basic linear single-degree-of-freedom (SDOF) system depicted in Fig. 1 (without the horizontal springs k_h) this parameter is defined as the modulus of the ratio between the force transmitted to the host structure (the base) (f_t) and the excitation force (f_e) or, in case of base excitation, as the ratio between the displacement (x_t) of the payload (m) and that of the base (x_e). For the linear case, force and displacement transmissibilities are the same and for both the mathematical expression is [1]

$$|T| = \left|\frac{f_t}{f_e}\right| = \left|\frac{x_t}{x_e}\right| = \sqrt{\frac{1+4\zeta^2\Omega^2}{(1-\Omega^2)^2+4\zeta^2\Omega^2}} \tag{1}$$

where $\zeta = c/2\sqrt{k_v m}$ is the damping ratio and $\Omega = \omega/\omega_n$ is the non-dimensional excitation frequency, with $\omega_n = \sqrt{k_v/m}$. From Eq. (1), two observations follow: (1) if the isolator is linear, force and displacement transmissibility are the same; and (2) in the idealised case of a mass supported on a linear isolator, transmitted vibrations are only attenuated at frequencies above the square root of two times the fundamental natural frequency of the system, i.e. $|T| < 1$ when $\Omega > \sqrt{2}$. Therefore, for a given mass, the frequency above which isolation can occur is governed by the stiffness of the

* Corresponding author. Now at: LMS International, Leuven 3100, Belgium.
E-mail address: A.Carrella@bristol.ac.uk (A. Carrella).

0020-7403/$ - see front matter © 2011 Elsevier Ltd. All rights reserved.
doi:10.1016/j.ijmecsci.2011.11.012

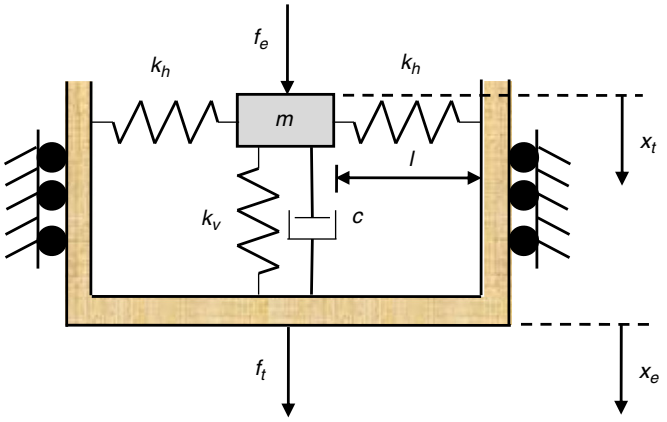

Fig. 1. Simple model of a nonlinear isolator that behaves as a Duffing oscillator at low amplitudes of excitation. The mass can either be excited by the excitation force f_e, with x_e set to zero, i.e. the foundation is rigid, or the foundation can be excited with an imposed displacement x_e and the force f_e is set to zero.

isolator and there is often a practical limitation on the minimum value of this.

Ideally, the isolator would have a high-static-stiffness – capable of bearing the load without much static displacement, and a low-dynamic-stiffness – which will provide the low natural frequency required for improved vibration isolation performance. This High-Static-Low-Dynamic-Stiffness (HSLDS) characteristic can be achieved using a nonlinear mount. A numerical analysis of nonlinear isolators, with reference to their transmissibility, is presented in [2–4]. The review paper by Ibrahim [5] compares many nonlinear isolators and shows that research in nonlinear isolators is a very active field. The work in Refs. [6–9] discusses some details of the HSDLS mechanism. Recently, Zhou and Liu have applied the HSLDS principle to a semi-active system in which a mechanical spring is coupled with a magnetic spring [10]. Robertson et al. also exploit magnets in order to engineer an isolation system with the desired HSDLS characteristic [11]. Zhang et al. have presented a paper [12] in which they investigate whether the nonlinear element should be the damper or the spring. In order to do so, the authors use a cubic stiffness and a cubic damper (i.e. the damping force is proportional to the cube of the velocity), but without providing indication of a physical model with this characteristics.

In this paper, first a simple model of a mechanical system with the desired nonlinear stiffness is presented. Some experimental work was also carried out in [13] to demonstrate the concept. Subsequently, the analysis and comparison of both force and displacement transmissibility, when the system is subject to harmonic excitation, is presented. To emphasise the relevant physical behaviour of the system rather than the mathematical aspects, it will be assumed that that the isolation mechanism behaves such that the displacements are small enough to be able to assume that the response is at the same frequency as the excitation. This is dependent upon the damping and the degree of nonlinearity in the isolator and so will vary on a case by case basis. In this paper the results are presented in a non-dimensional form, thus allowing the maximum allowable amplitude to be calculated for each specific case once the properties of the system are known. The assumption enables simplified closed-form solutions for the force and displacement transmissibilites to be derived in terms of non-dimensional parameters. It is recognised that for high amplitudes of excitation and for low levels of damping the system may exhibit other types of response, such as period doubling and chaos, as described in reference [14].

The model of the nonlinear HSLDS isolation system is shown in Fig. 1. One of the springs supports the mass and the other two springs, which are called corrector or auxiliary springs [13], act as a negative stiffness and thus control the natural frequency, and hence the frequency above which isolation occurs. This spring configuration mimics the force–deflection characteristic of many nonlinear isolators, shown for example in [5,15,16] and is thus a useful model to study the basic behaviour of this class of nonlinear isolator. This is the main aim of this paper. It is not the intention here to discuss and compare the advantages of the many different types of isolators, as this is done comprehensively in the review paper by Ibrahim [5] and the book by Riven [16]. Rather the intention is to use relatively simple analytical models to discuss some of the characteristics of force and base-excited systems with HSLDS isolators. Using the analytical expressions derived, the factors which govern the effectiveness of the isolators are discussed and reasons are given as to why the force and displacement transmissibilities differ for nonlinear isolators.

If the displacement of the three-spring isolator is small compared to its dimension then its force–deflection characteristic can be approximated by a cubic polynomial, thus forming a Duffing oscillator when a mass is placed on it. The study of the Duffing equation (free and forced response of a system with cubic stiffness) is ubiquitous in nonlinear dynamics [17]. In this work, focus is placed on the transmissibility functions. The simplified analytical expressions are derived using the well-established Harmonic Balance to a first-order expansion [18]. To confirm that the system behaves as assumed for the parameters used in the simulations, direct numerical integration of the equations of motion is carried out and the results compared with the analytical solutions.

2. Description of the nonlinear isolator

Fig. 1 shows a simple lumped parameter model of a nonlinear vibration isolation system, with vertical stiffness k_v and linear damping coefficient c, which is valid for low frequencies. The mass m, can either represent a machine excited by force f_e, or an item of equipment isolated from base excitation x_e. In the first case, it is assumed that the foundation is rigid so that $x_e=0$, and in the latter case the excitation force $f_e=0$. The system is very similar to the classic SDOF model found in basic text books, for example [1], but here two additional horizontal springs each with stiffness k_h are attached [15]. These springs have the effect of creating a nonlinear isolator that can be adjusted so that the linear natural frequency of the system is reduced. This occurs, because close to the static equilibrium position, the "horizontal" springs can act as a negative stiffness in the vertical direction [6]. In the system shown in Fig. 1, the force transmissibility, which is defined as the ratio of the amplitude of force transmitted to the rigid foundation to the amplitude of the excitation force (at the frequency of excitation), differs from the displacement transmissibility, which is defined as the ratio of the displacement amplitude of the mass to the amplitude of the excitation displacement (again at the frequency of excitation). This is in contrast to the case of a linear isolator in which the force and displacement transmissibility are the same.

The force–deflection curve for the isolator is given by

$$f = k_v x + 2k_h\left(1-\frac{l_o}{(x^2+l^2)^{1/2}}\right)x \tag{2a}$$

where x is the displacement from the static equilibrium position. Eq. (2a) can be written in non-dimensional form as

$$\hat{f} = \frac{f}{k_v x_s} = \hat{x} + 2\hat{k}\left(1-\frac{1}{(\hat{x}^2(1-\hat{l}^2)+\hat{l}^2)^{1/2}}\right)\hat{x} \tag{2b}$$

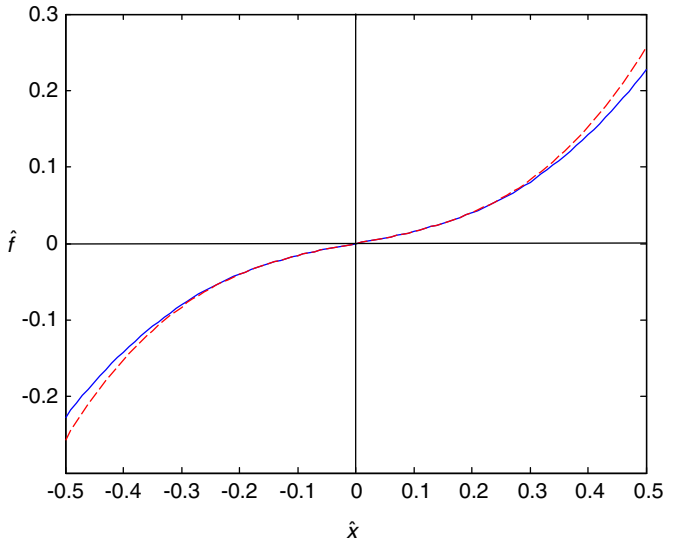

Fig. 2. Exact and approximate nonlinear restoring force as a function of non-dimensional displacement. Exact force given by Eq. (2), solid line. Approximate force given by Eq. (3), dashed line, $\hat{l}=0.7$.

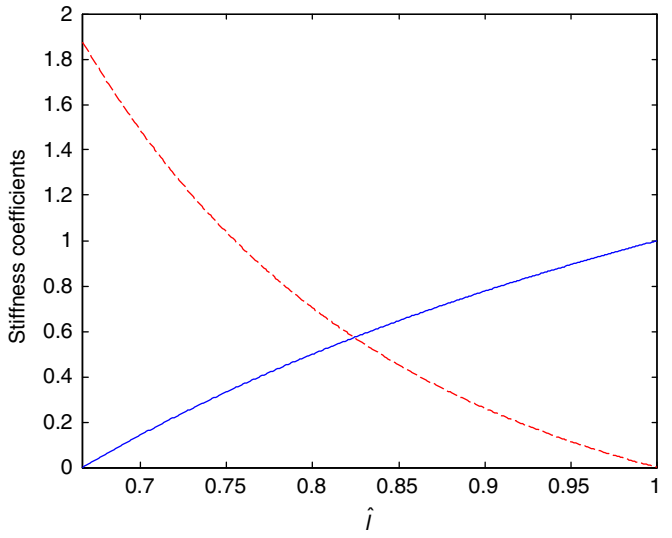

Fig. 3. Stiffness coefficients in the approximate model of the restoring force as a function of $\hat{l}$. The coefficient of the linear term, α, is given by the solid line, and the coefficient of the cubic term, γ, is given by the dashed line.

where $\hat{x}=(x/x_s)$, in which $x_s=(l_o^2-l^2)^{1/2}$ is the static deflection of the corrective springs, when the mass is placed onto it, such that its static equilibrium position is when the two springs k_h are horizontal as depicted in Fig. 1; $\hat{l}=(l/l_o)$, in which l_o is the free length of the lateral springs, l is their length when they are in the horizontal position and $\hat{k}=(k_h/k_v)$.

The two parameters that control the degree of geometric nonlinearity are $\hat{k}$ and $\hat{l}$. If $\hat{l}<1$, then the effect of the horizontal springs is to soften the isolator such that its stiffness is less than the vertical spring alone. If $\hat{k}=1$, then $\hat{l}$ must be greater than or equal to 2/3 in order that the stiffness of the isolator does not become negative and have a snap-through characteristic [6].

Eq. (2b) can be approximated by

$$\hat{f}=\alpha\hat{x}+\gamma\hat{x}^3 \tag{3}$$

where $\alpha=1-2\hat{k}((1-\hat{l})/\hat{l})$and $\gamma=\hat{k}((1-\hat{l}^2)/\hat{l}^3)$. Eqs. (2a) and (3), with $\hat{k}=1$, are plotted in Fig. 2 which shows that, provided the amplitude of the displacement is limited to about 0.4 of the static displacement, then the approximation given in Eq. (3) holds. The dimensional form of Eq. (3) is $f=k_1x+k_3x^3$, in which $k_1=k_v-2((l_o/l)-1)k_h$, and $k_3=(l_o/l^3)k_h$. It is clear that the horizontal springs have two effects; they reduce the linear stiffness so that it is smaller than the linear stiffness element k_v, and they introduce the cubic stiffness term k_3. The first effect is desirable as it decreases the linear natural frequency with a consequential increase in the vibration isolation region. The second effect is undesirable as it causes a hardening nonlinearity in the isolator, which results in the resonance peak bending to higher frequencies, potentially reducing the frequency range over which there is vibration isolation. The coefficients α and γ are plotted in Fig. 3 as a function of $\hat{l}$. It is clear from this graph that the penalty for reducing the linear stiffness is an increase in the nonlinearity.

3. Force transmissibility

For the system in Fig. 1, with $x_e=0$, the equation of motion for harmonic forced excitation is given by

$$m\ddot{x}+c\dot{x}+k_1x+k_3x^3=f_e=F_e\cos(\omega t) \tag{4}$$

Non-dimensionalising Eq. (4) gives

$$\hat{x}''+2\zeta\hat{x}'+\alpha\hat{x}+\gamma\hat{x}^3=\hat{F}_e\cos(\Omega\tau) \tag{5}$$

where $\hat{x}=(x/x_s)$, $\zeta=(c/2m\omega_n)$, $\omega_n=\sqrt{k_v/m}$, $\alpha=(k_1/k_v)$ $\gamma=(k_3x_s^2/k_v)$, $\Omega=(\omega/\omega_n)$, $\tau=\omega_n t$, $\hat{F}_e=(F_e/k_vx_s)$,with $(\cdot)'=(d(\cdot)/d\tau)$. Note that ω_n is the natural frequency of the system when the amplitude of oscillations are small enough so that the nonlinear term is negligible. Applying the Harmonic Balance (HB) method and assuming a solution of the form $\hat{x}=\hat{X}\cos(\Omega\tau+\phi_F)$, with the term containing $\cos 3\Omega\tau$ neglected, leads to the frequency–amplitude relationship

$$\left(\frac{3}{4}\gamma\hat{X}^3+(\alpha-\Omega^2)\hat{X}\right)^2+(2\zeta\Omega\hat{X})^2=\hat{F}_e^2. \tag{6}$$

This is a quadratic equation in Ω^2 which can be solved to give

$$\Omega_{1,2}\approx\sqrt{\frac{3}{4}\gamma\hat{X}^2+(\alpha-2\zeta^2)\pm\frac{1}{\hat{X}}\sqrt{\hat{F}_e^2-4\hat{X}^2\zeta^2}\left(\alpha-\zeta^2+\frac{3}{4}\hat{X}^2\gamma\zeta^2\right)} \tag{7a, b}$$

which are the two stable branches (also referred to as *resonant* and *non-resonant* branches) of the frequency response curve. The non-dimensional force transmitted through the nonlinear spring and the dashpot that comprises the isolator, is given by

$$\hat{f}_t=2\zeta\dot{\hat{x}}+\alpha\hat{x}+\gamma\hat{x}^3. \tag{8}$$

Using the HB method the component of the transmitted force at the excitation frequency has the form $\hat{f}_t=\hat{F}_t\cos(\Omega\tau+\varphi_T)$, where the magnitude of the force is given by

$$\hat{F}_t=\hat{X}\left(\left(\alpha+\frac{3}{4}\gamma\hat{X}^2\right)^2+4\zeta^2\Omega^2\right)^{1/2} \tag{9}$$

The force transmissibility is given by

$$|T_F|=\frac{\hat{F}_t}{\hat{F}_e} \tag{10}$$

Thus the magnitude of the transmissibility for the resonant and non-resonant branches can be determined by substituting for the two solutions for $\Omega_{1,2}$ given in Eq. (7) into Eq. (9) and

combining with Eq. (10) to give

$$|T_F|_1 = \frac{\hat{X}((\alpha+(3/4)\gamma\hat{X}^2)^2+4\zeta^2\Omega_1^2)^{1/2}}{\hat{F}_e} \tag{11a}$$

$$|T_F|_2 = \frac{\hat{X}((\alpha+(3/4)\gamma\hat{X}^2)^2+4\zeta^2\Omega_2^2)^{1/2}}{\hat{F}_e} \tag{11b}$$

The peak transmissibility corresponds to the peak displacement response, which can be determined by noting that Eq. (7a,b) are equal at this frequency, and hence $\hat{F}_e^2-4\hat{X}^2\zeta^2(\alpha-\zeta^2)-3\hat{X}^4\gamma\zeta^2=0$. Solving this equation gives

$$\hat{X}_{\max} = \left(\frac{2}{3\gamma}\left(\zeta^2-\alpha+\left(\frac{\zeta^3}{4}+\alpha(\alpha-2\zeta^2)+\frac{3\gamma\hat{F}_e^2}{4\zeta^2}\right)^{1/2}\right)\right)^{1/2} \tag{12}$$

Substituting Eq. (12) into Eqs. (11a) (or (11b)) and assuming that the damping is small so the term $4\zeta^2\Omega_1^2$, $(4\zeta^2\Omega_2^2)$is negligible compared to the other terms, yields

$$|T_F|_{\max} \approx \frac{1}{\sqrt{6\gamma}\hat{F}_e}\left(\zeta^2-\alpha+\left(\zeta^4+\alpha(\alpha-2\zeta^2)+\frac{3\gamma\hat{F}_e^2}{4\zeta^2}\right)^{1/2}\right)^{1/2} \times\left(\zeta^2+\alpha+\left(\zeta^4+\alpha(\alpha-2\zeta^2)+\frac{3\gamma\hat{F}_e^2}{4\zeta^2}\right)^{1/2}\right) \tag{13a}$$

Further, if $\zeta \ll 1$ this simplifies to

$$|T_F|_{\max} \approx \frac{1}{\sqrt{6\gamma}\hat{F}_e}\left(-\alpha+\left(\alpha^2+\frac{3\gamma\hat{F}_e^2}{4\zeta^2}\right)^{1/2}\right)^{1/2}\left(\alpha+\left(\alpha^2+\frac{3\gamma\hat{F}_e^2}{4\zeta^2}\right)^{1/2}\right) \tag{13b}$$

The frequency at which the transmissibility is a maximum can be calculated by substituting Eq. (12) into Eq. (7a) to give

$$\Omega_{F\max} = \frac{1}{\sqrt{2}}\left(\alpha-3\zeta^2+\left(\zeta^4+\alpha(\alpha-2\zeta^2)+\frac{3\gamma\hat{F}_e^2}{4\zeta^2}\right)^{1/2}\right)^{1/2} \tag{14a}$$

If $\zeta \ll 1$ this simplifies to

$$\Omega_{F\max} \approx \frac{1}{\sqrt{2}}\left(\alpha+\left(\alpha^2+\frac{3\gamma\hat{F}_e^2}{4\zeta^2}\right)^{1/2}\right)^{1/2} \tag{14b}$$

Eq. (13b) can be simplified and written in terms of $\Omega_{F\max}$. Note that Eq. (13b) can be written as

$$|T_F|_{\max} = \frac{1}{2\sqrt{2}\zeta}\left(\frac{4\zeta^2}{3\gamma\hat{F}_e^2}\right)^{1/2}(A^2-B^2)^{1/2}(A+B)^{1/2},$$

in which $A=(\alpha^2+(3\gamma\hat{F}_e^2/4\zeta^2))^{1/2}$ and $B=\alpha$. Thus, Eq. (13b) can be simplified to

$$|T_F|_{\max} \approx \frac{\Omega_{F\max}}{2\zeta} \tag{15}$$

The maximum force that can be applied such that the peak in the response occurs at $\Omega=1$ can be determined by rearranging Eq. (14a) to give

$$\hat{F}_{e\max} = \left(\frac{4\zeta^2}{3\gamma}((2+3\zeta^2-\alpha)^2-\zeta^4-\alpha(\alpha-2\zeta^2))\right)^{1/2} \tag{16a}$$

If $\zeta \ll 1$ this simplifies to

$$\hat{F}_{e\max} = 4\zeta\left(\frac{1-\alpha}{3\gamma}\right)^{1/2} \quad 0<\alpha<1 \tag{16b}$$

which shows that the maximum force that can be applied such that the peak in the transmissibility does not occur at frequencies greater than $\Omega=1$, increases as α decreases from unity and reaches a maximum of $4\zeta(1/3\gamma)^{1/2}$ when $\alpha=0$. Note that, for practical purposes, the maximum value of the excitation force given in Eq. (16b) can be taken as the maximum force for which the theory given in this paper is applicable. If the force exceeds this value then the system may not respond in accordance with the assumption made in the derivation of the expressions given above. This corresponds to the case when the linear stiffness is zero. The force transmissibility is plotted in Fig. 4 for various values of $\hat{l}$, in which the non-dimensional excitation force is set to $\hat{F}_{e\max}$ in each case. It can be seen that for each value of $\hat{l}$ the maximum occurs at $\Omega=1$ as expected. The force transmissibility is plotted in Fig. 5, again for various values of $\hat{l}$, but now the non-dimensional excitation force is set to the same value in each case.

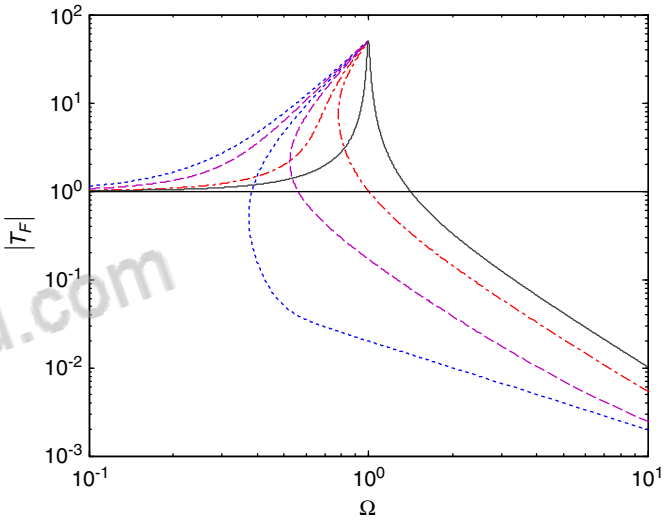

Fig. 4. Magnitude of the force transmissibility for different ratios of $\hat{l}$ and for $\zeta=0.01$. In each case, the force is set to $\hat{F}_{\max}$ so that the maximum value of the transmissibility occurs at $\Omega=1$. Solid line, $\hat{l}=1$; dashed-dotted line, $\hat{l}=0.8$; dashed line, $\hat{l}=0.7$; dotted line, $\hat{l}=2/3$.

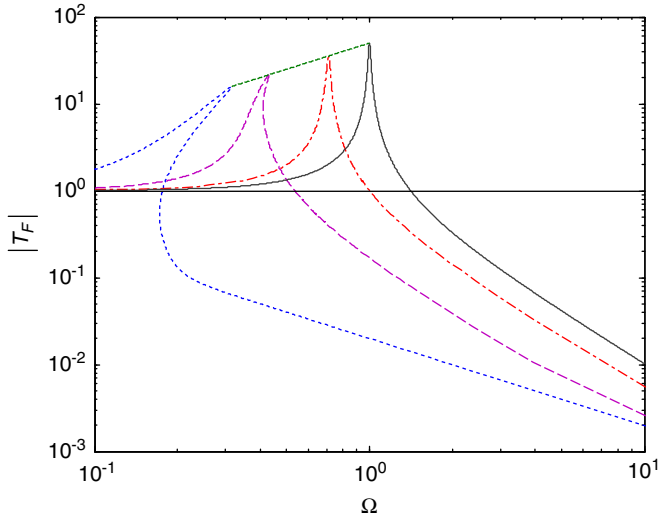

Fig. 5. Magnitude of the force transmissibility for different ratios of $\hat{l}$ and for $\zeta=0.01$. In each case, the force is set so $\hat{F}=0.1\ \hat{F}_{\max}|_{\alpha=0}$. Solid line, $\hat{l}=1$; dashed-dotted line, $\hat{l}=0.8$; dashed line, $\hat{l}=0.7$; dotted line, $\hat{l}=2/3$. The thin dashed line connecting the peaks is given by Eq. (15).

This is one tenth of the maximum when the linear term is set to zero, i.e. $0.1\hat{F}_{emax}|_{\alpha=0}$. Eq. (15) is also plotted to show that the locus of the peaks is described by this as α decreases from unity to zero. From Fig. 5 it can be seen that the frequency at which isolation occurs in each case is dependent upon how much the frequency response curve bends to the right. If the jump-down frequency occurs at a frequency greater than $\sqrt{2}\omega_n\alpha$ then when the frequency is increased from zero isolation occurs at the jump-down frequency. If the jump-down frequency occurs at a frequency lower than this, then isolation occurs at $\sqrt{2}\omega_n\alpha$. Clearly, the factors that affect this are $\hat{l}$, $\hat{F}_e$ and ζ. To illustrate some typical cases for a decreasing amplitude of excitation force the jump-down frequency is plotted as a function of $\hat{l}$ in Fig. 6. It can be seen that for $\hat{F}_e=0.01\hat{F}_{emax}|_{\alpha=0}$ and $\hat{F}_e=0.1\hat{F}_{emax}|_{\alpha=0}$ the isolation frequency occurs at $\Omega_l=\sqrt{2\alpha}$ for most values of $\hat{l}$, but when the excitation force is large, such that $\hat{F}_e=\hat{F}_{emax}|_{\alpha=0}$ then for $\hat{l}<0.8$ the non-linearity has sufficient strength to bend the curve to the right such that the isolation frequency occurs at the jump-down frequency.

It should be noted that the above analysis assumes steady-state behaviour of the system. In practice, the machine would be run up quickly to its operating speed. This means that the transmitted force would not reach the maximum amplitude given by Eq. (13a,b), and that the jump-down would not be as severe as in the steady-state prediction. Thus, the maximum transmissibility, given by Eq. (13a,b) is an upper bound, and is not likely to be reached in practice. If the jump-up and jump-down frequencies are of particular concern, then they can be avoided by setting the damping so that $\zeta \geq (3^{5/2}/2^8)^{1/3}\gamma^{1/3}$ [19].

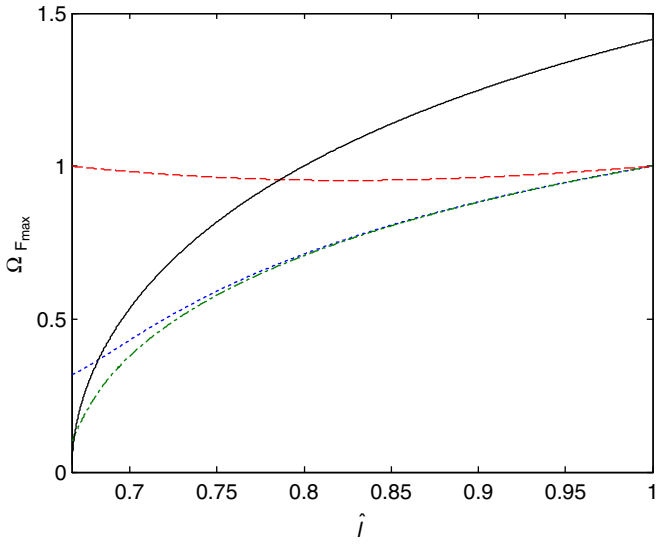

Fig. 6. Frequencies, $\Omega_{F\max}$, at which the peak in the force transmissibility occurs as a function of $\hat{l}$, for various amplitudes of the excitation force $\hat{F}$ and for $\zeta=0.01$. Dashed line, $\hat{F}=1$; dotted line, $\hat{F}=0.1$; dashed-dotted line, $\hat{F}=0.01$. The solid line given by $\Omega_l=\sqrt{2\alpha}$ is also shown for reference. If $\Omega_{F\max}\leq\Omega_l$, then isolation occurs at frequencies $\Omega>\Omega_l$. If $\Omega_{F\max}>\Omega_l$ then isolation occurs at frequencies $\Omega>\Omega_{F\max}$.

4. Displacement transmissibility

For the system in Fig. 1, with $f_e=0$, the equation of motion for harmonic displacement excitation of the base which is constant for each frequency, is given by

$$m\ddot{z}+c\dot{z}+k_1z+k_3z^3=m\omega^2X_e\cos(\omega t) \tag{17}$$

where $z=x_e-x_t$ is the relative displacement between the suspended mass and the base and X_e is the amplitude of the base displacement. Note that in this case that base excitation at frequency ω is equivalent to exciting the system with a force increasing with the square of frequency. Non-dimensionalising Eq. (17) gives

$$\hat{z}''+2\zeta\hat{z}'+\alpha\hat{z}+\hat{X}_e^2\gamma\hat{z}^3=\Omega^2\cos(\Omega\tau) \tag{18}$$

where $\hat{z}=(z/X_e)$, $\hat{X}_e=(X_e/x_s)$ and the other terms are as in the forced case described in the previous section. Applying the harmonic balance method and assuming a solution of the form $\hat{z}=\hat{Z}\cos(\Omega\tau+\phi_D)$, with the term containing $\cos 3\Omega\tau$ neglected, leads to

$$\frac{3}{4}\hat{X}_e^2\gamma\hat{Z}^3+(\alpha-\Omega^2)\hat{Z}=\Omega^2\cos\phi_D \tag{19a}$$

$$-2\zeta\Omega\hat{Z}=\Omega^2\sin\phi_D \tag{19b}$$

Squaring and adding Eq. (19a,b) gives the amplitude–frequency equation

$$\left(\frac{3}{4}\hat{X}_e^2\gamma\hat{Z}^3+(\alpha-\Omega^2)\hat{Z}\right)^2+(2\zeta\Omega\hat{Z})^2=\Omega^4 \tag{20}$$

As in the force excited case, this is a quadratic equation in Ω^2 which can be solved to give

$$\Omega_{1,2}\approx\left(\frac{\hat{Z}^2((3/4)\gamma\hat{X}_e^2\hat{Z}^2+\alpha-2\zeta^2)\pm\hat{Z}(((3/4)\gamma\hat{X}_e^2\hat{Z}^2+\alpha)((3/4)\gamma\hat{X}_e^2\hat{Z}^2+\alpha-4\hat{Z}^2\zeta^2)+4\hat{Z}^2\zeta^4)^{1/2}}{\hat{Z}^2-1}\right)^{1/2} \tag{21a,b}$$

The maximum response can be determined by setting the inner radicand in Eq. (21a,b) to zero, to give

$$\hat{Z}_{\max}=\left(\frac{((3\alpha\gamma\hat{X}_e^2/4\zeta^2)+2\zeta(\zeta+(\alpha/\zeta)))-2\zeta((3\alpha\gamma\hat{X}_e^2/4\zeta^2)+(\zeta-(\alpha/\zeta))^2)^{1/2}}{3\gamma\hat{Y}^2(1-(3\gamma\hat{X}_e^2/16\zeta^2))}\right)^{1/2} \tag{22}$$

Note that Eq. (22) will have an unbounded response if $(3\gamma\hat{X}_e^2/16\zeta^2)\geq 1$ [6,20]. This is in contrast with the linear case in which any amount of damping in the isolator will result in a bounded response. The relative displacement transmissibility is given by $T_r=\hat{Z}$. The resonant and non-resonant branches of the absolute displacement transmissibility curve are given by

$$|T_D|_{1,2}=(1+2\hat{Z}\cos\phi_{D(1,2)}+\hat{Z}^2)^{1/2} \tag{23}$$

where $\cos\phi_D$ is determined from Eq. (19a). The maximum response can be determined by setting the inner radicand in Eq. (21a,b) to zero, and noting that the maximum response occurs approximately when $\cos\phi_D=0$, so that if $\hat{Z}_{\max}^2\gg 1$ then

$$|T_D|_{\max}\approx\hat{Z}_{\max} \tag{24a}$$

Letting $\zeta\ll 1$, and noting the fact that $3\gamma\hat{X}_e^2/16\zeta^2$ must be less than unity for a bounded response, Eq. (24a) can be combined with Eq. (22) which can be significantly simplified to give

$$|T_D|_{\max}\approx\frac{1}{2\zeta}\left(\frac{\alpha}{1-(3\gamma\hat{X}_e^2/16\zeta^2)}\right)^{1/2} \tag{24b}$$

which occurs at a frequency of

$$\Omega_{D\max}\approx\left(\frac{\hat{Z}_{\max}^2((3/4)\gamma\hat{X}_e^2\hat{Z}_{\max}^2+\alpha-2\zeta^2)}{\hat{Z}_{\max}^2-1}\right)^{1/2} \tag{25a}$$

where $\hat{Z}_{\max}$ is given by Eq. (22). Making the same assumptions as in the derivation of (24b) an approximate expression can be determined for $\Omega_{\max}$, which is

$$\Omega_{D\max} \approx \left(\frac{\alpha}{1-(3\gamma\hat{X}_e^2/16\zeta^2)}\right)^{1/2} \tag{25b}$$

As in the case for forced excitation a simple expression relates the maximum transmissibility, the frequency at which this occurs, and the damping. This can be determined by combining Eqs. (24b) and (25b) to give

$$|T_D|_{\max} \approx \frac{\Omega_{D\max}}{2\zeta} \tag{26}$$

The maximum input displacement that can be applied such that the peak in the response occurs at $\Omega=1$ can be determined by rearranging Eq. (25b) to give

$$\hat{X}_{e\max} = 4\zeta\left(\frac{1-\alpha}{3\gamma}\right)^{1/2} \quad 0<\alpha<1 \tag{27}$$

which has the same form as for the maximum force given in Eq. (16b), and the same restrictions on the amplitude of excitation apply. Thus, the larger the nonlinearity and hence the smaller the value of α, the larger the base displacement can be before the transmissibility peaks at a frequency greater than that for the system without the horizontal springs.

Fig. 7 shows the absolute displacement transmissibility for various values of $\hat{l}$ when the displacement excitation is set to a maximum as given by Eq. (27) such that the peaks in all the responses occur at a frequency of $\Omega=1$. It can be seen that, qualitatively, the curves have a different shape than those for the force transmissibility shown in Fig. 4. Fig. 8 shows the displacement transmissibility when the displacement is set so that $\hat{X}_e = 0.9\hat{X}_{\max}|_{\alpha\approx 0}$. The line joining the peaks together given by Eq. (26) is also plotted. It can again be seen that the curves are qualitatively different from the force transmissibility, and that the horizontal springs are extremely effective in reducing the linear natural frequency of the system, thus increasing the range of frequencies over which isolation can occur.

Fig. 9 shows the jump-down frequencies as a function of $\hat{l}$ for different levels of excitation. This is compared with the isolation frequency for a linear system $\Omega_l = \sqrt{2\alpha}$ as for the forced case in Fig. 6.

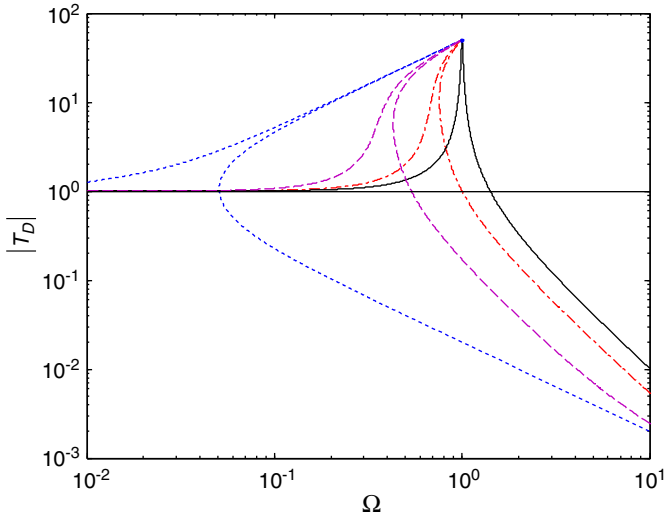

Fig. 7. Magnitude of the displacement transmissibility for different ratios of $\hat{l}$ and for $\zeta=0.01$. In each case, the base displacement is set to $\hat{X}_{\max}$ so that the maximum value of the transmissibility occurs at $\Omega=1$. Solid line, $\hat{l}=1$; dashed-dotted line, $\hat{l}=0.8$; dashed line, $\hat{l}=0.7$; dotted line, $\hat{l}=0.667$.

It can be seen that, for base excitation, the undesirable effect of bending the frequency response curve to the right for a given geometric nonlinearity is more pronounced than for forced excitation. Accordingly for many values of α and $\hat{X}_e$the minimum frequency at which isolation is the jump-down frequency rather than Ω_l.

As in the case of force excitation this frequency and the severity of the jump-down are likely to much less in practice as machines are generally run up to their operating speed quickly.

5. Comparison of force and displacement tranmissibility

In Sections 3 and 4 explicit expressions for the force and displacement transmissibility were derived. It is clear that these

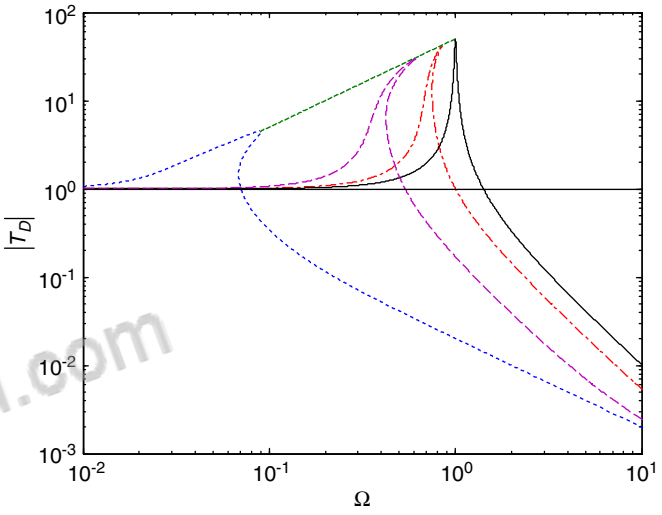

Fig. 8. Magnitude of the displacement transmissibility for different ratios of $\hat{l}$ and for $\zeta=0.01$. In each case, the base displacement is set to be constant with frequency such that $\hat{X}_e = 0.9\hat{X}_{\max}|_{\alpha\approx 0,\hat{l}=2/3}$. Solid line, $\hat{l}=1$; dashed-dotted line, $\hat{l}=0.8$; dashed line, $\hat{l}=0.7$; dotted line, $\hat{l}=0.667$. The thin dashed green line connecting the peaks is given by Eq. (26).

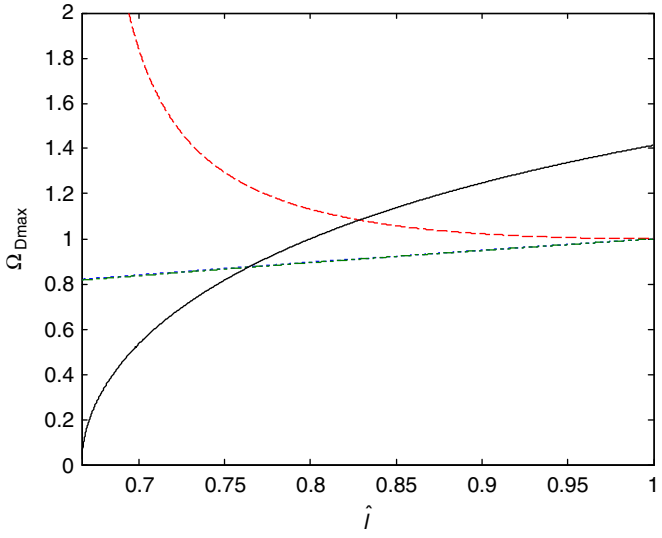

Fig. 9. Frequencies, $\Omega_{D\max}$, at which the peak in the displacement transmissibility occurs as a function of $\hat{l}$, for various amplitudes of the base excitation $\hat{X}_e$ and for $\zeta=0.01$. Dashed line, $\hat{X}_e = \hat{X}_{e\max}|_{\alpha\approx 0}$; dotted line, $\hat{X}_e = 0.1\ \hat{X}_{e\max}|_{\alpha\approx 0}$; dashed-dotted line, $\hat{X}_e = 0.01\ \hat{X}_{e\max}|_{\alpha\approx 0}$(this is not noticible as it overlays with the dotted line). The solid line given by $\Omega_l = \sqrt{2\alpha}$ is also shown for reference. If $\Omega_{D\max} \le \Omega_l$ then isolation occurs at frequencies $\Omega > \Omega_l$. If $\Omega_{D\max} > \Omega_l$ then isolation occurs at frequencies $\Omega > \Omega_{D\max}$.

are different, unlike in the linear case, because they are dependent on the amplitude of excitation, which is a force in one case and a displacement in the other. In this section they are compared by choosing a particular value of excitation. Moreover the expressions are checked for certain parameter values by direct numerical integration of the equation of motion.

To compare the force and displacement transmissibility, the amplitude of base excitation was chosen to be $\hat{X}_e = 0.9\hat{X}_{\max}|_{\alpha\approx 0,\hat{l}=2/3}$ and for the force excitation the force was chosen such that the displacement was the same as this at zero frequency. The results are plotted in Fig. 10. in which the transmissibility and frequency have linear axes, so that they can be easily compared. Numerical results are also plotted as circles. Note that the numerical results are the amplitude of the first harmonic; the maximum amplitude of the higher harmonics was less than 5% of the first harmonic. It is clear from the comparison with the numerical results that the expressions for the transmissibilities are reasonably accurate for the parameters given. The difference between the force and displacement transmissibilities is also clear. For values of $\hat{l}$ close to 2/3 the force tranmissibility bends more to the right, but as $\hat{l}$ increases the nonlinear effect on the displacement transmissibility is more pronounced than that on the force transmissibility. All the peaks, however, in both the force and displacement transmissibility are on the same straight line given by Eqs. (15) or (26). The force and the displacement transmissibilities for the nonlinear case will only be the same if the force applied to the mass is the same as the product of the mass and the acceleration of the base, which is clear from the comparison of Eqs. (5) and (17). This condition is unimportant for the linear system because the transmissibility is not a function of the excitation amplitude. However, it is important for the nonlinear system. Thus the *force* transmissibility and the *acceleration* transmissibility would be the same for the nonlinear system shown in Fig. 1, but the displacement transmissibility in which the base displacement is the same at each frequency is not. The displacement transmissibility would only be the same as the force transmissibility if the base acceleration is kept the same at each frequency. It is clear from Fig. 10 that the displacement transmissibility is affected by the nonlinearity more as frequency increases.

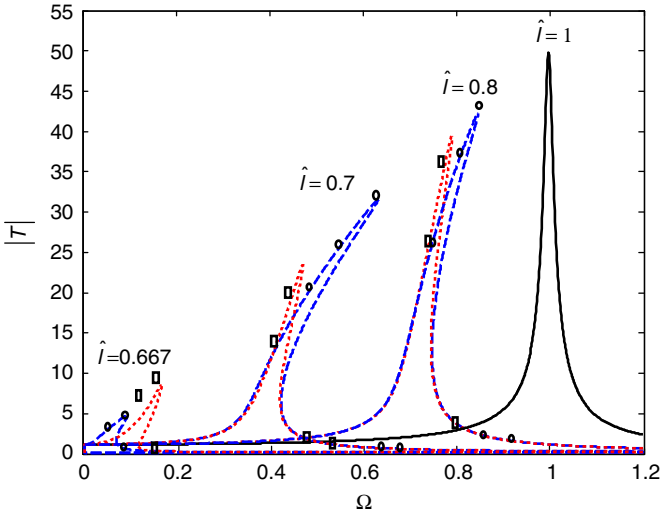

Fig. 10. Comparison of the force and displacement transmissibilities for different values of $\hat{l}$ (shown on linear axes for clarity) and for $\zeta=0.01$. In each case the displacement of the mass at zero frequency is set to be the same, $\hat{X}_e = 0.9\ \hat{X}_{\max}|_{\alpha\approx 0,\hat{l}=2/3}$, which means that the force is different for each value of $\hat{l}$, but the base displacement is constant with frequency. The dashed lines are for $|T_D|$, and the dotted lines for $|T_F|$. The squares and circles are the results of direct numerical integration of the equation of motion.

This is because by keeping the base displacement constant, the base acceleration increases with frequency and hence the nonlinearity has a greater effect. This is the reason why the maximum amplitude increases without bound if $(3\gamma\hat{X}_e^2/16\zeta^2)\geq 1$. To illustrate this, consider the jump down frequency of the forced case when $\alpha=1$. If $(3\gamma\hat{F}_e^2/4\zeta^2)\ll 1$ Eq. (14b) can be simplified to

$$\Omega_{F\max}^2 \approx 1+\frac{3\gamma\hat{F}_e^2}{16\zeta^2} \tag{28}$$

Note that for the base-excited case this is also true provided that the excitation force is not constant but increases with frequency as $\hat{F}_e=\Omega^2\hat{X}_e$. Thus Eq. (28) can be written as

$$\Omega_{D\max}^2 \approx 1+\frac{3\gamma\Omega_{D\max}^2\hat{X}_e}{16\zeta^2} \tag{29}$$

which can be rearranged to give the same as Eq. (25b) with $\alpha=1$. Thus it is because the effect of the nonlinearity increases with frequency because of the increasing base acceleration with frequency that causes the difference between the jump-down frequencies in the force and the base-excited systems.

6. Conclusions

Common measures of the effectiveness of an isolator at low frequencies are the force and displacement transmissibilities. In this paper, expressions of these two quantities have been derived for a single degree-of-freedom system containing a nonlinear stiffness element. The stiffness element consists of three springs, one of which provides a positive stiffness (the main spring) and two other springs (auxiliary springs) act as a negative stiffness close to the static equibrium position. This spring configuration mimics the force–deflection characteristic of many nonlinear isolators. By adjusting the properties of the auxiliary springs (the stiffness or the length), the linear natural frequency can be reduced so that the frequency range over which isolation occurs can be increased. However, as the linear natural frequency reduces the nonlinearity increases, which is an undesirable effect. This is less pronounced if the amplitude of the excitation is small. To enable analytical solutions to be derived, the stiffness element was approximated so that the force deflection characteristic could be described by a linear and a cubic term. The resulting system behaved as a hardening Duffing oscillator.

Unlike a linear isolator, in which the force and displacement transmissibilities are the same, for the system with the nonlinear isolator studied in this paper, this is not so. This is because the nonlinearity depends upon the relative displacement across the isolator and this is only the same for the force and base-excited systems if the acceleration of the base is kept constant at each frequency. Thus, the force and the acceleration transmissibilities are the same, but if the base-excited system has a constant displacement amplitude input at each frequency then the acceleration increases with frequency, and so the effect of nonlinearity also increases with frequency, resulting in a displacement transmissibility which is different from the force transmissibility.

References

[1] Rao SS. Mechanical vibrations. 4th Edition. Peason Education; 2003.
[2] Ravindra B, Mallik AK. Hard Duffing-type vibration isolators with combined Coulomb and viscous damping. International Journal of Nonlinear Mechanics 1993;28(4):427–40.
[3] Ravindra B, Mallik AK. Performance of non-linear vibration isolators under harmonic excitation. Journal of Sound and Vibration 1994;170(3):325–37.
[4] Nakhaie Jazar G, Houim R, Narimarani A, Golnaraghi MF. Frequency response and jump avoidance in a nonlinear passive engine mount. Journal of Vibration and Control 2006;12(11):1205–37.
[5] Ibrahim RA. Recent advances in nonlinear passive vibration isolators. Journal of Sound and Vibration 2008;314:371–452.

[6] Carrella A. Passive vibration isolators with high-static-low-dynamic stiffness. PhD thesis. ISVR, University of Southampton; 2008.
[7] Carrella A, Brennan MJ, Waters TP. Static analysis of a passive vibration isolator with Quasi-Zero Stiffness Characteristic. Journal of Sound and Vibration 2007; 301(3–5):678–89.
[8] Carrella A, Brennan MJ, Kovacic I, Waters TP. On the force transmissibility of a vibration isolator with quasi-zero stiffness. Journal of Sound and Vibration 2009;322(4–5):707–17.
[9] Kovacic I, Brennan MJ, Waters TP. A study of a nonlinear vibration isolator with quasi-zero stiffness characteristic. Journal of Sound and Vibration 2008; 315(3):700–11.
[10] Zhou N, Liu K. A tunable high-static–low-dynamic stiffness vibration isolator. Journal of Sound and Vibration 2010;329:1254–73.
[11] Robertson Will S, Kidner MRF, Cazzolato Ben S, Zander Anthony C. Theoretical design parameters for a quasi-zero stiffness magnetic spring for vibration isolation. Journal of Sound and Vibration 2009;326(1–2):88–10325 2009;326: 88–103.
[12] Zhang B, Billings SA, Zi-Qiang L, Tomlinson GR. Suppressing resonant vibrations using nonlinear springs and dampers. Journal of Vibration and Control 2009; 15(11):1731–44.
[13] Carrella A, Brennan MJ, Waters TP. A demonstrator to show the effects of negative stiffness on the natural frequency of a simple oscillator. Proceedings of the Institution of Mechanical Engineers, Part C: Journal of Mechanical Engineering Science 2008;222(7):1189–92.
[14] Moon FC. Chaotic vibrations: an introduction for applied scientists and engineers. Wiley VCH; 2004.
[15] Alabuzhev P, Gritchin A, Kim L, Migirenko G, Chon V, Stepanov P. Vibration protecting and measuring systems with quasi-zero stiffness. NY: Hemisphere Publishing; 1989.
[16] Rivin EI. Passive vibration isolation. ASME Press; 2001.
[17] Kovacic I, Brennan MJ. The Duffing equation: nonlinear oscillators and their behaviour. Wiley; 2011.
[18] Jordan DW, Smith P. Nonlinear ordinary differential equations: an introduction to dynamical systems. 3rd ed. Oxford University Press.
[19] Brennan MJ, Kovacic I, Carrella A, Waters TP. On the jump-up and the jump-down frequencies of the Duffing oscillator. Journal of Sound and Vibration 2008;318(4–5):1250–61.
[20] Milovanovic Z, Kovacic I, Brennan MJ. On the displacement transmissibility of a base excited viscously damped nonlinear vibration isolator. Transactions of the ASME Journal of Vibration and Acoustics 2009;131(5). Article Number: 054502.